International Journal of Engineering & Technology, 7 (4.7) (2018) 356-360

International Journal of Engineering & Technology

Website: www.sciencepubco.com/index.php/IJET

Research paperResearch Paper

Concrete Surfacing Using Surface Energy of Nanoparticles

Anastasia Sychova[1], Larisa Svatovskaya[2*], Dmitriy Starchukov[3], Vassily Gera[4], Maxim Sychov[5]

[1]*Doctor of Technical Sciences, Professor of the Department of «Special Complexes and Systems», Military Space Academy named after A.F. Mozhaysky, Zhdanovskaya st. 13, Saint-Petersburg, Russia. Email: amsychova@yandex.ru*
[2]*Doctor of Technical Sciences, Head of the Department of «Engineering chemistry and natural science», Emperor Alexander I St.Petersburg State Transport University (PGUPS), Moskovsky pr., 9, Saint-Petersburg, Russia. Email: lbsvatovskaya@yandex.ru*
[3]*Candidate of Technical Sciences, Associate Professor of Department of «Special facilities of rocket and space complexes», Military Space Academy named after A.F. Mozhaysky, Zhdanovskaya st. 13, Saint-Petersburg, Russia. Email: starchukov@mail.ru*
[4]*Candidate of Technical Sciences, Head of Department of «Engineering and Electromechanical support», Military Space Academy named after A.F. Mozhaysky, Zhdanovskaya st. 13, Saint-Petersburg, Russia. Email: geratv33@mail.ru*
[5]*Doctor of technical sciences, Head of Department of «Theoretical base of the materials», Petersburg State Technology Institute (Technical University), Moskovsky pr., 26, Saint-Petersburg, Russia.*
**Corresponding author E-mail: msychov@yahoo.com*

Abstract

This article considers scientific and practical principles of concrete surfacing. As it was found, such production can be done by impregnating the surface of high-strength concrete with silica sol, measuring the surface energy of nanoparticles introduced. A technique was introduced for calculating surface energy of sols, so was the range of energy necessary to create concrete with a shock resistant surface, determined by measurement and calculation. The content contains possible reactions resulting in new phases in the concrete top during the impregnation with silica sol. Physical and mechanical characteristics of surfaced concrete were also outlined ad considered, so were the XRD data and electron microscopy data. Various types of energy used to surface concrete until high dynamic strength were compared. This article provides evidence that surface energy of sol nanoparticles can be considered as an independent alternative source.

Keywords: *surfaced concrete, silica sol, surface energy, concrete impregnation, surface hardiness.*

1. Introduction

These days there is a range of materials with a shock resistant surface [1-3]. Those include armor ceramics made of different materials [4-6]. The most effective ceramics from boron carbide [7; 8]. Among other things, armor steel is widely used [9; 10], so as materials from aluminum alloys [11; 12]. Yet, such material as concrete with high dynamic strength has no scientific and practical grounds for production applications. Unlike other materials, concrete with high dynamic strength has a lower density, so the final product made out of it will be lighter and cheaper to produce. This is important for assessing its economic efficiency, since a high-quality armor ceramics are an expensive sphere of manufacturing. At the same time, a cement stone can be considered as a ceramic material good for making materials suitable for armored barriers.

Ceramics generally respond to deformable impactors penetrating their surface at high speed in two stages [27]. At the first stage, minimum penetration rates arise from and the maximum rates of impactor deformation (shortening). As the damage caused to ceramics progresses, penetration parameters change and transform the product into a loose medium. At the second stage, penetration rate is close to being equal, and its value corresponds to penetration into material with zero strength. This means that penetration resistance is tied at this stage to inertia forces. The ballistic effect of ceramics obviously depends on fist-case penetration parameters, considering the maximum penetration resistance displayed in the first case. Destruction kinetics of ceramics and their behavior upon impact depend both on the intensity of that impact (velocity at collision and impactor density) and on the physical and mechanical properties of ceramics [28]. However, the problem of what properties materials should have to ensure a ballistic effect of ceramic product remains open. Since the typical impactor-to-target geometry ratio is such that the impactor is somewhat smaller than the target, the compression wave from the impactor reaches the free surface first and bounces off as a rarefaction wave. As a result, a shock wave and a rarefaction wave propagating one after the other generate a compression pulse of finite width. When a shock wave reflects from the target surface, a second rarefaction wave occurs, and the superposition of two rarefaction waves gives a tension stress so that local interiors in the target go negative in pressure. In spallation, local destruction occurs and some part of material just breaks away [29].

The common ideas about the physics and mechanics of ceramic specimen destruction at high-velocity collision with solid bodies have not been clearly articulated yet. However, theoretical research and trials show that effective performance of armor ceramics is linked to several factors (optimum density of material, high modulus of elasticity, hardness, crack resistance, expected strength and velocity of propagating longitudinal elastic wave. From the full-scale data and results of mainstream use of combined multilayer material (armor ceramics in combination with polymeric installations), which was used for armoring purposes in many countries, we can claim the combination of a high-strength surface with a high-strength installation over it to be the optimal armored barrier. The frontal layer of combined obstacles must

have a high dynamic strength to stand energy dynamic loads, while the installation must minimize damage occurrence behind the tiles.

The purpose of this research is to introduce an armored barrier configuration from cement-concrete stone with rational strength properties and economic characteristics.

Concrete with a shock-resistant surface can be made from high-strength concrete by strengthening the entire volume of the cube [13-15] or by surfacing it [16].

Dynamic strength criteria of various materials can be measured by the following formula, $(GPa \cdot m)^3 \cdot K/kg$ [17]:

$$M=EH_K\sigma_bT_m/\rho \quad (1)$$

Where: E – modulus of elasticity, GPa; H_K – Knoop hardness, GPa, σ_b – breaking point, MPa; T_m – melting point, K; ρ – density, g/cm^3.

From (1), it follows that surface hardiness is one of the important properties of material with shock resistant surface [17; 18].

From this perspective, concrete surfacing is a more advisable technique to use of making product with high dynamic strength.

The use of sols (colloidal solutions containing nanoparticles of 1-100 nm in size) is one of the known methods for cement activation [19-21]. In surface hardening, concrete is impregnated with organic silicious fluids, gunite, and otherwise. Yet, silica sols were not used in concrete surface hardening applications.

Research hypothesis is that production of concrete with a shock resistant surface, defied as surface with high dynamic strength, required additional energy to be introduced, such as surface energy of sol nanoparticles.

High surface energy of nonoinclusions generates multiple centers of crystallization in maturing concrete stone. Trials indicated that monocrystalline samples have the highest dynamic strength [29].Single crystals, however, have dynamic strength dependent on defects in the crystal structure, such as dislocations. A crystalline body is being made more strong typically by eliminating those dislocations through minimization of crystal count. With a dislocation density known, crystallite with a size below the inverse dislocation density may not have dislocations at all and have a strength close to an abstractive point. Thus, if the number of crystals embedded in a concrete stone is multiple, they can form a layer of high microhardness. Nanoparticles, due to their size, have huge amounts of surplus surface energy, which they seek to release. This energy can be introduced into the concrete by saturation with sols. This will activate the hardening process and promote the chemical reaction between the components inside the fresh concrete, improving surface characteristics.

Among that, sol particles of choice must interact with the concrete components, resulting in new solid phases. These formations should appear mainly in hollow areas of concrete (pores), improving its hardness and strength properties. At this point, phases will form a solid high-strength layer of a certain thickness, let us call it a casing, which will perform a shock resistance function (Figure 1). This surfacing technique will give a high dynamic strength of concrete surface.

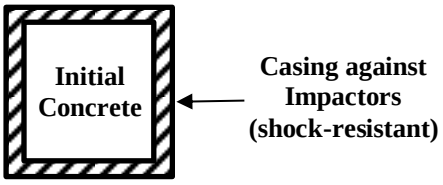

Fig. 1: Surfaced Concrete: Inner Hardened Formation in a Casing

The advantage of such a casing is that it eliminates a compositional structure of a single concrete block: two layers are different in hardness, strength and thicknesses, but there is no phase interface between them.

Concrete surface impregnation must be performed in an enveloping fashion to exclude concrete fragments flying away in different directions at collision. This effect is typical for concrete, which is basically a brittle material. This is a bad news for those, who random flying fragments may hit. Generated casing with high-strength facets will 'hold' the concrete, preventing it from cracking and exploding the cracked off parts in different directions.

Below are theoretical provisions, which enable surfacing of concrete with non-organic sols until high dynamic strength of its surface, if met.

Provision 1

In exothermic hydration of cement, a huge amount of energy is released into the environment as heat during the first seconds of the process (Figure 2) [22]. Because of that, additional energy from nanoparticles will be an over boost that can prevent the cement fraction from activating.

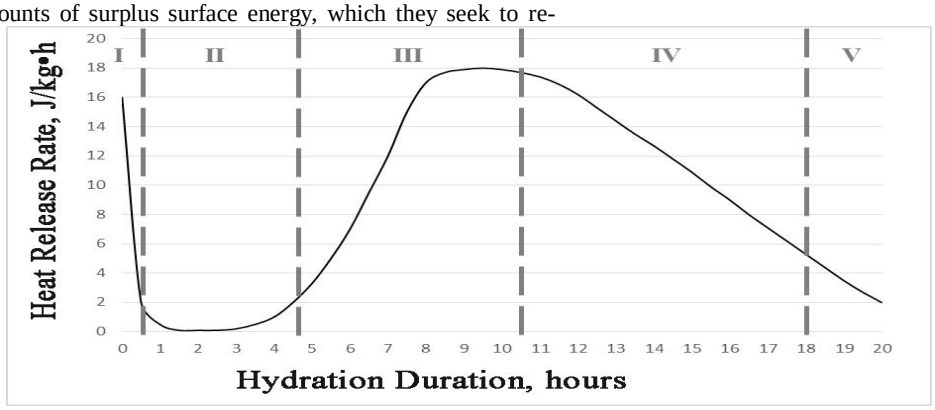

Fig. 2: The Rate of Hydration in $3CaO–SiO_2$ System; I, II, III, IV – Heat Generation Stages

This assumption fits the Le Chatelier's principle: when a system in equilibrium experiences a disturbance (such as temperature or pressure changes), then the equilibrium will shift in the direction that counteracts the change imposed (principle of counteraction).

In our case, cement systems will respond to additional surface energy introduced by shifting in the direction of slowing down the hydration.

Hence, sols should be introduced to the cement system at a time when the rate of heat release is reduced and the major amount of thermal energy is released, which is a 20-hours follow-up, approximately (Figure 2). This is when the reaction will involve most of the sol and cement components, resulting in the generation of new phases. This will provide a concrete with improved surface (increased hardness, improved strength and other enhanced physical and mechanical characteristics).

If the above assumptions are correct, then there is some kind of a window in the range of surface energy amounts to introduce, within which the nanoparticles will activate the cement hardening process. This window can be found by measuring the

amount of surface energy of sol nanoparticles introduced into the system (Figure 3) [22, 23].

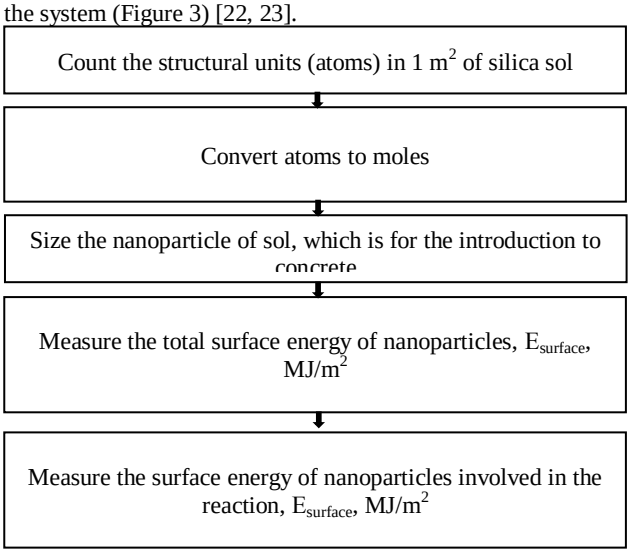

Fig. 3: Steps to Measure the Surface Energy of Sol Nanoparticles

Provision 2

In hydration, calcium hydrosilicates form (CaO/SiO_2), which are responsible for the strength of the cement stone and the concrete, naturally.

The low-base calcium hydrosilicates (C/S <1.2) give better hardness and strength properties (Tables 1, 2) [24].

Table 1. Relationship between Compressive Strength and Hydrosilicate Alkalinity

№	Hydrosilicates	Alkalinity		Compressive Strength, MPa
		CaO/SiO_2	*Name*	
1	$C_2SH(A)$	2	High-Base	2.1
2	C_6S_6H	1	Low-Base	12.5
3	$C_5S_6H_5$	0.8	Low-Base	17.5

Table 2. Relationship between Hardness and Hydrosilicate Alkalinity

№	Hydrosilicates	Alkalinity		Moh's Hardness
		CaO/SiO_2	*Name*	
1	$C_4S_3H_3$	1.3	High-Base	3
2	$C_3S_2H_3$	1.5	High-Base	4
3	$C_3S_6H_6$	0.5	Low-Base	5
	C_6S_6H	1	Low-Base	6.5

From this, it follows that concrete surface with high dynamic strength forms due to the generation of low-base calcium hydrosilicates in its layer. This can be achieved by introducing nanoparticles of a certain soil.

Table 3 shows reactions that can result in solid phases forming in the surface layer of concrete at various stages of hardening.

Reactions 3-7 can give new phases in the surface layer of concrete, if it was impregnated with silica sol. Silica sol was the trial solution of choice because of its known positive effect on cement systems at activation.

Table 3: Possible Reactions Resulting in the Formation of Solid Phases in the Top Layer of Hardening Concrete

Reaction Number	Hardening Process as Chemical Reaction
	Primary Reactions
1	$3CaO{\cdot}SiO_2+3H_2O \rightarrow 2CaO{\cdot}SiO_2{\cdot}2H_2O+Ca(OH)_2$
2	$2(2CaO{\cdot}SiO_2)+3H_2O \rightarrow 3{,}3CaO{\cdot}2SiO_2{\cdot}2{,}3H_2O+0{,}7Ca(OH)_2$
	Side Reactions with Silica Sol
3	$Ca(OH)_2+SiO_2{\cdot}H_2O \rightarrow 2CaO{\cdot}SiO_2{\cdot}1{,}17H_2O+1{,}83H_2O$
4	$2CaO{\cdot}SiO_2{\cdot}1{,}17H_2O + 2(SiO_2{\cdot}H_2O) \rightarrow 2CaO{\cdot}3SiO_2{\cdot}2{,}5H_2O\ (C_2S_3H_{2,5}) + 0{,}67H_2O$
5	$Ca(OH)_2+2(SiO_2{\cdot}H_2O) \rightarrow CaO{\cdot}2SiO_2{\cdot}2H_2O+H_2O$
6	$6Ca(OH)_2+6(SiO_2{\cdot}H_2O) \rightarrow 6CaO{\cdot}6SiO_2{\cdot}H_2O\ (C_6S_6H)+11H_2O$
7	$5Ca(OH)_2+6(SiO_2{\cdot}H_2O) \rightarrow 5CaO{\cdot}6SiO_2{\cdot}5{,}5H_2O\ (C_5S_6H_5)+5{,}5H_2O$

In top layer, hydration efficiency can be improved through the following spontaneous physicochemical processes:

- increase in the amount of cement components in reaction and minimization of hydrosilicate alkalinity (reaction 4);
- reaction between $Ca(OH)_2$, which is the output of reactions 1 and 2, and low-base calcium hydrosilicates (reactions 3, 5-7);
- acceleration of hardening processes.

2. Experiment

Below are experimental results of making concrete with a shock-resistant surface. The experiment was performed on high-strength concrete with 800 (kg/cm^2) strength. Composition of the basic mix is shown in Table 4.

Table 4: Composition of the Basic Mix of Concrete with 800 (kg/cm^2) Strength

Portion in 1 m^3 of Concrete Mix, kg				
Cement	Sand	Gravel	Water	Workability
520	662	1036	202	Mix P2 Level

For concrete production, the following materials were used:

– Portland cement M400 D20 (CEM II A/SH 32.5);
– Sand (FM 2.26);
– Gravel (5 to 10 mm fraction);
– Water (GOST 23732-79).

Samples were impregnated with 3% silica sol, which penetrated inside the prepared concretes through the pore channels.

Void-to-cement ratio changes with cement hardening to a maximum value at 1-day age or so [22]. Hence, surfacing process should be done at this age of concrete. At the same time, technological features of concrete production indicate that finished concrete product must have strength high enough for further transportation and impregnation with sol (2- or 3-day age).

Impregnation with silica sol was performed for 3 days. Then, concrete specimens were kept 28 days under normal conditions of hardening (at 20 ± 2°C and 95% RH).

Physical and technical characteristics of produced concrete are shown in Table 5.

Table 5: Quality Characteristics of Surfaced Concrete

Indicator	Surfaced Specimen	Increment, % relative to Original
Moh's Hardness	7	75
Compressive Strength	69.9 MPa	78
Flexural Strength	9.2 MPa	76
Elasticity Modulus	52 $MPa{\cdot}10^{-3}$	37
Abrasion Resistance	0.67 g/cm^2	25
Water Resistance	1.4 MPa	75
Frost Resistance	600 cycles	200
Water Absorption	1.9 %	60

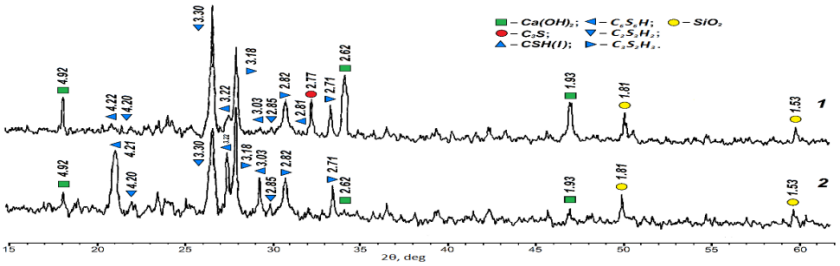

Fig. 5: XRD data on Cement Stone:1 – prior to surfacing; 2 – subsequent to surfacing

Figure 5 shows findings of the X-ray phase analysis of concrete specimens impregnated with silica sol. The $Ca(OH)_2$ and C_3S phases are present only in the original concrete, there is no footprint of them in the surfaced sample [25]. This indicates that $Ca(OH)_2$ reacts with silica sol particles resulting in new formations (Table 3), while C_3S steps into effective hydration, improving the hardening process. This process fits the earlier theoretical provisions.

Aside from that, roentgenogram displays lines that correspond to low-base hydrosilicates, such as C_6S_6H, $C_2S_3H_2.5$, and $C_3S_2H_3$, which occurrence was also expected (Table 3).

The electron microscopy revealed that new phases were generated in the voids (up to 1 cm in length) of the surface layer of concrete, clogging them. From this, it follows that concrete surface impregnation gives a layer with high hardiness and high dynamic strength. This layer acts as a non-organic solid casing, which speaks in favor of the previously stated assumptions.

The lack of $Ca(OH)_2$ footprints, which are the major cause of cement stone corrosion, and high physical and mechanical properties of obtained concrete indicate high corrosion resistance and durability of the resulted product.

3. Results and Discussion

Table 6 shows how the concentration of silica sol used to surface the concrete is tied to the calculated value of surface energy, $E_{surface}$, and sample hardness, *H*.

The surface energy of silica sol nanoparticles (particle size 22 nm) was calculated according to the methodology in Figure 4.

Table 6: Relationship between Calculated Surface Energy and Concrete Hardiness

№	Sol Concentration, %*	Portion of Colloid SiO_2 involved in Reaction, kg/m^3*	Surface Energy, $E_{surface} \cdot 10^{-10}$, kJ/m^3	Hardiness, GPa
1	0.75	0.175	1.8	1.6
2	1.5	0.35	3.6	2.1
3	3	0.7	7.2	2.4
4	6	1.4	14.4	2.1
5	9	2.8	28.8	1.8

*Note: * – calculated with regard to total mass of sol absorbed by the concrete, 23 kg/m³*

Data in the Table 6 show an increasing trend in concrete surface hardiness with the increasing amount of SiO_2 involved in the reaction, and naturally, with the increasing amount of surface energy introduced. An excessive amount of energy at the surface of concrete has a negative effect on hydration. Thus, assumptions made in [19] are received evidence. At this point, the window in the range of input energy, which will give a maximum boost to cement hardening process, is probably between 2 and $14.4 \cdot 10^{10}$ kJ/m^3. The best casing solution can be achieved at $7.2 \cdot 10^{10}$ kJ/m^3.

Table 5 shows a 75% increase in compressive strength and a 78% increase in flexural strength of concrete after impregnation, while other characteristics were boosted up to 200%.

Table 7 shows dynamic strength criteria (*M*) for various materials (armor ceramics from boron carbide, armor steel and trial concrete), their applications and cost. Thus, *M* criteria for armor steel and armor ceramics are not the same, and the trial concrete differs from them by times. The cost of concrete is three orders of magnitude lower than that of armor ceramics and two orders of magnitude lower than that of armor steel. Concrete with high dynamic strength can be used in essential constrictions for destruction proofing.

Table 7: Comparative Cost-Performance Data on Shock-Resistant Materials

Material	Dynamic Strength Criterion, M, $(GPa \cdot m)^3 \cdot K/kg$	Application	Cost, RUB/kg
Hot-pressed Boron Carbide B_4C	$5.3 \cdot 10^3$	In armchairs and flight control systems for helicopters	9000
Armor Steel	$0.5 \cdot 10^3$	In weapons and military equipment, metal-concrete mattress coatings	801
Concrete with High Dynamic Strength	$0.01 \cdot 10^3$	In essential construction for destruction proofing	3.1

The findings that were made from the experiment allowed designing an energy-saving technology of surface hardening for concrete with a view of forming a solid high-strength casing improving the properties of concrete (abrasion resistance, frost resistance, water absorption).

On a final note, Table 8 shows comparative data on different types of energy used in practice, which enable the production of high-strength concrete at a cement basis.

Data in the Table show that surface energy of nanoparticles is the only effective and affordable form of energy that can be introduced to concrete for strengthening purposes. Hence, this kind of energy can be considered as an independent and alternative source.

Table 8: Comparative Data on Different Types of Energy used in High-Strength Concrete Production

Characteristics	Concrete Treatment		
	Steam Curing	***Autoclave Curing***	***Surfacing***
Energy	*Thermal*		*Surface*
Gross Energy, kJ/m^3	$1 \cdot 10^6$	$5 \cdot 10^6$	$7 \cdot 10^{10}$
Fuel Equivalent Cost, RUB/m^3	270	892	116*
Surface with High Dynamic Strength	–	–	+

*Note: * – cost of silica sol, which was absorbed by the concrete at impregnation*

4. Conclusions

1. This is the first research that coins a technology for producing concrete with high dynamic strength by surfacing with silica sol.
2. This is the first attempt to use surface energy of sol nanoparticles for activation of cement hardening process (calculation method provided).
3. This article provides science-based grounds for the introduction of surface energy of sol nanoparticles into the surface layer of concrete after 20 hours of cement hardening, due to active heat release during this period.
4. This is the first time when a safe window in the range of surface energy for introduction was found; for concrete with high dynamic strength at the surface, the optimum amount of surface energy to introduce is $7.2 \cdot 10^{10}$ kJ/m^3.
5. A comparative analysis of various types of energy used to produce high-strength concrete revealed that surface energy of nanoparticles is the only effective and affordable form of energy that can be introduced to concrete for strengthening purposes. Hence, this kind of energy can be considered as an independent and alternative source.

References

[1] Schuster, B. E., Aydelotte, B. B., Leavy, R. B., Satapathy, S., & Zellner, M. B. (2015). Concurrent velocimetry and flash x-ray characterization of impact and penetration in an armor ceramic. *Procedia Engineering*, *103*, 553-560.

[2] Grujicic, M., Pandurangan, B., Angstadt, D. C., Koudela, K. L., & Cheeseman, B. A. (2007). Ballistic-performance optimization of a hybrid carbon-nanotube/E-glass reinforced poly-vinyl-ester-epoxy-matrix composite armor. *Journal of materials science*, *42*(14), 5347-5359.

[3] Silnikov, M. V., Vasilyev, N. N., Spivak, A. I., Barkov, D. D. (2018). The method of obtaining bulletproof material from ballistic fabric. *Military Enginery Series: Counter-terrorism technical devices, 9*, 104-107.

[4] Huang, F. L., & Zhang, L. S. (2007). Investigation on ballistic performance of armor ceramics against long-rod penetration. *Metallurgical and Materials Transactions A*, *38*(12), 2891-2895.

[5] Coleman, S. P., Hernandez-Rivera, E., Behler, K. D., Synowczynski-Dunn, J., & Tschopp, M. A. (2016). Challenges of engineering grain boundaries in boron-based armor ceramics. *JOM*, *68*(6), 1605-1615.

[6] Zhitnyuk, S. V., Makarov, N. A., & Guseva, T. V. (2014). New silicon carbide based ceramic armor materials. *Glass and ceramics*, *71*(1-2), 6-9.

[7] Galanov, B. A., Kartuzov, V. V., Grigoriev, O. N., Melakh, L. M., Ivanov, S. M., Kartuzov, E. V., & Swoboda, P. (2013). Penetration resistance of B4C-CaB6 based light-weight armor materials. *Procedia Engineering*, *58*, 328-337.

[8] Kremenchugsky, M. V., Savkin, G. G., Malinov, V. I., Rachkovsky, A. I., Smorchkov, G. Yu. (2008). Ultra-light armored ceramic materials from nanostructured powders of boron carbide. *Rossijskie nanotehnologii [Russian Nanotechnologies]*. *3(3-4), 141*-146.

[9] Banerjee, A., Dhar, S., Acharyya, S., Datta, D., & Nayak, N. (2017). Numerical simulation of ballistic impact of armour steel plate by typical armour piercing projectile. *Procedia engineering*, *173*, 347-354.

[10] Bester, J. N., & Stumpf, W. E. (2013). Plasticity and Ballistic Characterization of a New Armour Steel. In *Dynamic Behavior of Materials, 1* (pp. 109-122).

[11] Artsruni, A. A., Tsurgozen, L. A., Makhov, B. F. (2010). Aluminum and problems of armor protection. In the Recent Problems of Protection and Safety. Proceedings of the 13th All-Russian Scientific and Practical Conference. Armored Vehicles and Weapons. *Russian Academy of Missile and Artillery Sciences (RARAN), 3*, 95-102.

[12] Gasqueres, C., Nissbaum, J. (2011). Ballistic performance and failure mode of high performance 2139-T8 and 7449-T6 Aluminium alloys, *26th International Symposium on Ballistics. Miami, September 12-16*, 1289-1295.

[13] Svatovskaya, L., Sychova, A., Sychov, M., Okrepilov, V. (2016). Quality Improvement of Concrete Articles. *MATEC Web of Conferences 53, 01023.*

[14] Sychova, A. M., Svatovskaya, L. B., Mjakin, S. V., Vasiljeva, I. V. (2009). Modification of fillers for cements (Book Chapter). *Electron Beam Modification of Solids: Mechanisms, Common Features and Promising Applications, 4.* 35-37.

[15] Sychova, A. M., Svatovskaya, L. B., Mjakin, S. V., Vasiljeva, I. V. (2009). Activation of aqueous phase at cement and concrete solidification (Book Chapter). *Electron Beam Modification of Solids: Mechanisms, Common Features and Promising Applications, 5*, 39-47.

[16] Starchukov, D. S., Kozin, P. A., Stepanova, I. V., Mandritsa, D. P., Ishakov, Sh. Sh., Kovalev, F. E. (2014). Engineering and chemical fundamentals behind the production of high-strength concrete with sol-containing additives: a monograph. *A.F. Mozhaysky's Military-Space Academy*, 108.

[17] Zaytsev, G. P. (2012). Corundum armor ceramics: production and application. Expert Union. 3. Electronic resource: http://www.unionexpert.ru/index.php/news/item/287-alumina-bronekeramika-experience-of-production-and-use

[18] Eliseev, V. S., Kravchenko, A. D., Yarosh, V. V. (2001). Ballistic effect of high-hard materials. *Military Enginery Series: Composite non-metal materials in mechanical engineering, 3-4*, 15-26.

[19] Svatovskaya, L., Kabanov, A., & Sychov, M. (2017). Soling, Aerating and Phosphating for Soil Strengthening and Detoxication. *Procedia engineering*, *189*, 398-403.

[20] Svatovskaya, L., Kabanov, A., & Sychov, M. (2017). Lithosynthesis of the properties in the transport construction on the cement base. In *IOP Conference Series: Earth and Environmental Science*, *90(1)*, p.12

[21] Svatovskaya, L., Urov, O., & Kabanov, A. (2017). Geoecoprotective technology of transport construction using silica sol absorption method. *Procedia engineering, 189*, 454-458.

[22] Butt, Yu. M., Sychev, M. M., Timashev, V. V. (1980). Chemical technology for binders. *Moscow: Vysshaya shkola*, 472.

[23] Shabanova, N. A., Sarkisov, P. D. (2004). Fundamentals of nanodispersed sol-gel technology. *Akademkniga Publishing House*, 208.

[24] Babushkin, V. I., Matveyev, G. M., Mchedlov-Petrossyan, O. P. (1986). Thermodynamics of silicates: 4th Edition [updated and revised]. *Moscow: Stroiizdat*, 408.

[25] Gorshkov, V. S., Timashev, V. V., Saveliev, V. G. (1981). Physical and chemical analysis of binders. *Moscow: Vysshaya shkola*, 336.

[26] Van Damme, H. (2018). Concrete material science: Past, present, and future innovations. *Cement and Concrete Research*.

[27] Vlasov, A. S. (2004). High-speed penetration into silicon carbide ceramics with different porosity. *Journal of Technical Physics, 74(5)*, 62-65

[28] Vlasov, A. S. (1999). Kinetics of high-speed penetration into high brittle media. *Solid State Physics, 41(10)*, 1785-1787.

[29] Antoun, T., Curran, D. R., Seaman, L., Kanel, G. I., Razorenov, S. V., & Utkin, A. V. (2003). *Spall fracture*. Springer Science & Business Media.